

## Polarization transfer in n-p scattering at 50 MeV

H. L. Woolverton,\* S. Nath, J. C. Hiebert, L. C. Northcliffe, and W. F. Woodward<sup>†</sup>  
*Cyclotron Institute, Texas A&M University, College Station, Texas 77843*

(Received 4 February 1985)

The polarization transfer parameter  $D_t(180^\circ)$  for n-p scattering has been measured at 50 MeV for the first time. Polarized neutrons produced in the  ${}^2\text{H}(\vec{d}, \vec{n}){}^3\text{He}$  reaction were scattered from the hydrogen in a polyethylene target and the polarization of the recoil protons emitted at  $0^\circ$  was measured in a carbon polarimeter. The result of this measurement tests the prediction of  $D_t$  from a phase shift analysis of the N-N data and that of a theoretical proposal concerning n-p charge exchange.

### I. INTRODUCTION

The details of the nucleon-nucleon (N-N) interaction have been studied using neutron-proton (n-p) or proton-proton (p-p) scattering for many years. Cross sections, both differential and total, analyzing powers, polarizations, spin-transfer, and spin-correlation parameters have been measured with ever increasing precision providing a more complete description of the scattering process in terms of the scattering matrix. Although the  $T=1$  N-N phase shifts are determined fairly accurately from the vast pool of precise p-p data, the  $T=0$  phase parameters are known with less accuracy because of the inherent lack of precision associated with the n-p data. For example, the  ${}^3\text{S}_1$ - ${}^3\text{D}_1$  mixing parameter  $\epsilon_1$  once was very poorly determined.<sup>1</sup> This parameter has been shown<sup>1</sup> to be quite sensitive to certain spin-correlation and spin transfer observables. Experimentally, the polarization transfer parameter  $D_t$  and the spin-correlation parameter  $C_{nn}$  (or its time-reversed equivalent  $A_{yy}$ ) are among the most feasible to measure. While  $A_{yy}$  has been measured at 50 MeV (Ref. 2) and incorporated into a phase shift analysis, thereby reducing the uncertainty in  $\epsilon_1$ , a measurement of  $D_t$  could be useful in further restricting this parameter.

The peaking of the n-p cross section in the backward-angle charge exchange region is still not clearly understood. Although it is probable that the sharp peak at very backward angles is due to one-pion exchange (OPE), the OPE amplitude in Born approximation produces a dip instead of a peak. Explanations of the backward peaking including either interference between the OPE amplitude and some sort of background of uncertain origin<sup>3</sup> or absorption corrections<sup>4</sup> to the OPE amplitude have not been completely successful. In an attempt to explain this discrepancy, Gibbs and Stephenson<sup>5</sup> proposed a theoretical scheme which involved an additional pseudoscalar term in the pion-nucleon vertex function. Their approach succeeded in predicting the low energy behavior of the  $\pi$ -p elastic scattering amplitude within experimental error. A measurement of  $D_t$  for n-p elastic scattering at  $180^\circ$  center of mass angle was suggested as a definitive test of this theory, and the value of  $D_t$  was predicted to be  $+0.7$  at 50 MeV. This is in sharp contrast with the phase-shift analysis prediction of  $D_t(180^\circ) = -0.16 \pm 0.03$  at 50 MeV. In this paper, a measurement of  $D_t(180^\circ)$  for n-p scatter-

ing at 50 MeV with a level of accuracy sufficient to distinguish between these two predictions is reported. This is the first such measurement in this energy region.

### II. EXPERIMENTAL DETAILS

The experiment was carried out at the Texas A&M polarized neutron facility, which is described in detail in Ref. 6. Here, only the details which are pertinent to the measurement will be given.

Three nuclear reactions were involved in the primary experiment. First, the  ${}^2\text{H}(\vec{d}, \vec{n}){}^3\text{He}$  reaction was used to produce polarized neutrons. These neutrons then bombarded a polyethylene target where the  $\vec{n}-\vec{p}$  scattering occurred. Finally,  $\vec{p}-\text{C}$  elastic scattering was used to determine the polarization of the outgoing  $0^\circ$  protons. A fourth reaction,  ${}^3\text{He}(\vec{d}, \vec{p}){}^4\text{He}$ , was used in the calibration of the p-C polarimeter.

The deuteron beam from an atomic-beam polarized ion source<sup>7</sup> was injected axially into the cyclotron, accelerated, magnetically analyzed, and transported to the target area. The beam polarization was monitored continuously in a polarimeter located upstream of the target area, by measuring the asymmetry in  $\vec{d}-\text{C}$  elastic scattering from a propane gas target. The value of the  $\vec{d}-\text{C}$  analyzing power was determined earlier at this laboratory<sup>8</sup> by comparing the asymmetry in  $\vec{d}-\text{C}$  scattering with that in  $\vec{d}-{}^4\text{He}$  scattering at the same energy, the analyzing power for the latter reaction being known.<sup>9</sup> The average vector polarization of the deuteron beam was  $0.464 \pm 0.04$  in the first set of runs and  $0.505 \pm 0.01$  for the second running period.

A schematic diagram showing the experimental setup in the target area is given in Fig. 1. The beam first passed through the secondary-emission monitor (SEM), in which the current of secondary electrons from a thin foil in the path of the beam was integrated to give a relative measurement of beam current. The device was calibrated between runs by insertion of a deep Faraday cup to collect the beam just downstream of the monitor. An electrostatic guard ring inhibited the exchange of electrons between the foil and the cup. With the Faraday cup withdrawn, the beam passed through the neutron production target  $T$ , a high-pressure ( $\sim 21$  atm) liquid-nitrogen-cooled target cell<sup>6</sup> of thickness  $\sim 6.35$  cm filled with deuterium. The

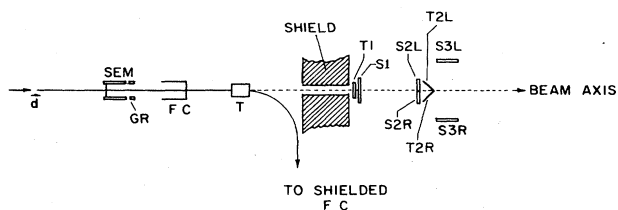


FIG. 1. Schematic diagram of the experimental setup, showing a secondary electron emission monitor (SEM), guard ring (GR), removable Faraday cup (FC), n-production target (*T*), polyethylene n-p conversion target (*T1*), carbon scatterer (*T2L-T2R*), and plastic scintillators (*S1, S2L, S2R, S3L, S3R*).

mean beam energy at the center of the target was 49.8 MeV. Beyond the target, a 90° bending magnet swept away charged particles and directed the emerging deuteron beam into a heavily shielded Faraday cup. The neutrons from the reaction passed through a collimator channel at 0°. The n-p target *T1* was a polyethylene slab of 6.4 mm thickness placed at the exit of the collimator, covering the entire aperture. Polyethylene was selected for its relatively high hydrogen to carbon ratio. The thickness was chosen as a compromise, to maximize the counting rate while limiting the energy spread of the recoil protons to ~8 MeV. The estimated probability per incident neutron for n-p scattering to produce a proton recoiling into the solid angle of 3.5 msr subtended by the carbon scatterer of the polarimeter was  $3 \times 10^{-6}$ .

Protons scattered near 0° were analyzed in a carbon polarimeter (*S2-T2-S3*), shown schematically in Fig. 1 and pictorially in Fig. 2. The carbon scatterer consisted of

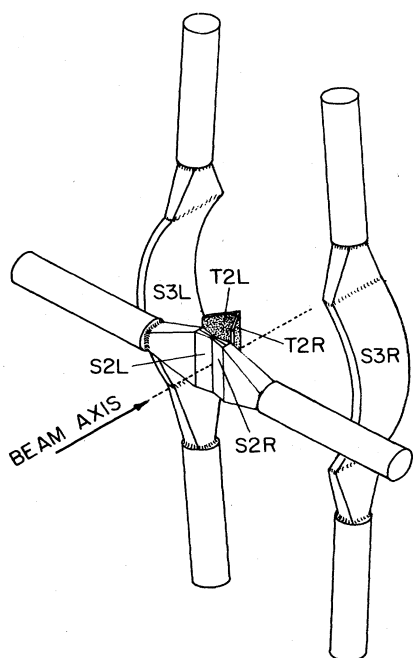


FIG. 2. Pictorial view of the carbon polarimeter-detector system with the supporting frames removed. Symbols have the same meaning as indicated in Fig. 1.

two slabs of graphite *T2L* and *T2R*, 3.2 mm in thickness, mounted as two sides of an equilateral triangle and placed 1.15 m from the n-p target. This particular geometry was chosen to increase the volume of carbon seen by incident protons, resulting in increased yield, while decreasing the amount of material in which rescattered protons lose energy before reaching the side detectors *S3L* and *S3R*. The third side of the equilateral triangle consisted of two sheets of NE102 plastic scintillator ( $3.4 \times 7.3$  cm<sup>2</sup>) *S2L* and *S2R* of thickness 0.5 mm butted together and viewed from the side by photomultiplier tubes (PMT's), as shown in Fig. 2. These pieces of NE102 were placed inside aluminized Mylar tents<sup>10</sup> which reflected the light through air light guides to the PMT's. Detectors *S2L* and *S2R* defined left and right scattering, respectively, provided time of flight (TOF) and pulse height information, and, incidentally, some additional *C* target material. This division of the carbon target into *S2L-T2L* and *S2R-T2R* makes the effective (n,p) center of mass scattering angle 179°. In order to ensure that the n-p events occurred in target *T1* and not *T2*, another detector (*S1* in Fig. 1) consisting of a thin (0.5 mm) NE102 scintillator mounted inside an aluminized Mylar tent was placed just downstream of the n-p target *T1*.

The left and right detectors *S3L* and *S3R* were large slabs ( $41.9 \times 12.7 \times 1.3$  cm<sup>3</sup>) of NE102, heat formed to have a 26.7 cm radius. As shown in Fig. 2, the configuration of these detectors was cylindrical and concentric to the beam axis so that, for a given polar scattering angle, protons of the same energy would have the same TOF for any azimuthal scattering angle. Each formed a quarter section of a right circular cylinder, subtending polar scattering angles ranging from 55° to 75° and azimuthal scattering angles from -45° to +45° (relative to the horizontal plane). Light was collected at both the top and bottom ends through Lucite light pipes, optically coupled to the PMT's. The choice of  $65^\circ \pm 10^\circ$  for the scattering angle was based on the fact that the figure of merit  $P^2I$  is large and roughly uniform<sup>11</sup> over this angular range.

### III. MEASUREMENT AND ANALYSIS

#### A. Neutron polarization

The value of the neutron polarization was determined on the basis of a stripping model.<sup>9,12</sup> Simmons *et al.*<sup>12</sup> first proposed that the vector polarization transfer parameter  $K_y^p(0^\circ)$  could be predicted by calculating the average spin polarization of the neutrons in the incident deuteron beam and assuming it to be unchanged by the stripping reaction. If a 6% *D*-state component in the deuteron wave function is assumed, the calculated value of  $K_y^p(0^\circ)$  is 0.607.<sup>9</sup> A refined calculation,<sup>13</sup> incorporating results obtained with both vector and tensor polarized incident deuterons, yields  $K_y^p(0^\circ) = 0.615$ . Evidence that the simple stripping model used to calculate  $K_y^p(0^\circ)$  is valid at high energies was presented in Ref. 14. In particular, the validity of this model is supported by the measured value,  $K_y^p(0^\circ) = 0.618 \pm 0.031$  for the charge symmetric reaction  ${}^2\text{H}(\vec{d}, \vec{p}){}^3\text{H}$  at 50.6 MeV.<sup>15</sup> The assumption that such a calculation is valid not only for the monoenergetic neutron group for the  ${}^2\text{H}(\vec{d}, \vec{n}){}^3\text{He}$  reaction but also for the

high-energy portion of the breakup neutron spectrum has been clearly supported by measurements from this laboratory<sup>16</sup> and from Karlsruhe<sup>17</sup> as well as in a measurement<sup>18</sup> of  $K_y'(0^\circ)$  for the  $^1\text{H}(\vec{d}, \vec{n})2\text{p}$  reaction. With the value of  $K_y' = 0.615$  the polarization  $P_n$  of the neutrons is

$$P_n = \frac{3}{2} P_d K_y' = 0.922 P_d. \quad (1)$$

For a typical value of  $P_d = 0.50$ , the neutron beam polarization, as given by Eq. (1), was  $P_n = 0.46$ , known with about the same uncertainty as  $P_d$ .

### B. Polarimeter calibration

In order to determine the polarization of the forward scattered n-p protons it is necessary to know the effective analyzing power  $A_y(\text{eff})$  of the polarimeter. In principle, a value for  $A_y(\text{eff})$  could be calculated for the geometry of the polarimeter from known values<sup>19,20</sup> of the p-C elastic analyzing power and differential cross section but this would necessitate resolving p-C elastic events from the inelastic events, reducing further the already very low yield. A more practical and reasonable way is to calibrate the polarimeter, i.e., to measure the effective left-right asymmetry for all p-C scatterings detected with an incident proton beam of known polarization. In order to calibrate the system at the same energy at which the  $D_i$  data were taken, it is necessary that the average energy of the protons in  $S1$  be 50 MeV. Because of the large energy loss (primarily in the wall of the vacuum chamber in the  $90^\circ$  magnet) this would have required 53.5 MeV protons from the cyclotron, and such a beam was not available during the experiment. As an alternative, therefore, monoenergetic protons from the reaction  $^3\text{He}(\vec{d}, \vec{p})^4\text{He}$  were used as the source of polarized protons. The calibrations were done without changing the incident primary polarized deuteron beam in any way, by removing the n-p target ( $T1$ ), changing the deuterium gas in  $T$  to  $^3\text{He}$ , turning off the  $90^\circ$  bending magnet and inserting an aluminum degrader of appropriate thickness so as to provide 50 MeV protons while stopping the deuterons. The polarization  $P_p(^3\text{He})$  of the protons was calculated on the basis of the stripping model described above, using Eq. (1), and from the measured asymmetry  $\epsilon(^3\text{He})$  the effective analyzing power  $A_y(\text{eff})$  was determined by means of the relation

$$A_y(\text{eff}) = \epsilon(^3\text{He}) / P_p(^3\text{He}). \quad (2)$$

The measured effective analyzing power was  $A_y(\text{eff}) = 0.35 \pm 0.02$ .

### C. Data taking procedure

Seven parameters were obtained for each event and stored on magnetic tape. They were the following:  $t1$ , the relative TOF from the target cell to  $S1$  (timed with respect to the cyclotron rf signal);  $t2$ , the TOF from  $S1$  to  $S2L$  or  $S2R$  where  $L$  and  $R$  designate left and right, respectively;  $t3_{\text{bot}}$ , the TOF from  $S2L$  to  $S3L$  or from  $S2R$  to  $S3R$  with the signal coming from the bottom PMT;  $t3_{\text{top}}$ , as for  $t3_{\text{bot}}$ , but with the signal coming from the top PMT; and the pulse height signals  $E1$ ,  $E2$ , and  $E3$  from  $S1$ ,  $S2$ , and  $S3_{\text{bot}} + S3_{\text{top}}$ , respectively. A tag word

was also recorded in order to identify which detectors were involved in each event. Valid events were triple coincidences, specifically  $S1 \cdot S2L \cdot S3L$  or  $S1 \cdot S2R \cdot S3R$ .

Data were collected in three phases, calibration of the p-C polarimeter with the polarized protons from the  $^3\text{He}(\vec{d}, \vec{p})^4\text{He}$  reaction, collection of the n-p  $D_i$  data using the  $^2\text{H}(\vec{d}, \vec{n})^3\text{He}$  neutrons and the polyethylene target for  $T1$ , and determination of the background contribution due to  $\text{C}(\vec{n}, \vec{p})$  reactions by replacement of  $T1$  with a sheet of graphite of thickness 4.0 mm. This thickness was chosen to give an energy loss equivalent to that for the protons scattered in the polyethylene, so that events due to  $\text{C}(n,p)$  reactions would appear at the same place in the spectra as the n-p events from the polyethylene target. Compensation for differences in the number densities of the two targets was achieved by normalizing the results.

Data were taken in four-run cycles, each run being labeled spin up ( $\uparrow$ ) or spin down ( $\downarrow$ ) to indicate the spin orientation of the incident deuteron beam, with the sequence being either ( $\uparrow\downarrow\uparrow$ ) or ( $\downarrow\uparrow\downarrow$ ). Before and after each run a foil monitor calibration was made. Due to the low counting rate for the n-p data, possible time shifts were investigated by removing the triple coincidence requirement and looking at the "doubles" data, i.e.,  $S1 \cdot S2L$  or  $S1 \cdot S2R$ , between cycles.

The essential features of the spectra obtained with the  $^3\text{He}(\vec{d}, \vec{p})$  protons in the calibration runs and the  $^2\text{H}(\vec{d}, \vec{n})$  neutrons in the n-p runs were the same. Both reactions produced a "monoenergetic" peak at an energy adjusted to be the same, as well as a continuum spectrum of breakup nucleons which was very similar for the two reactions. The data from both reactions were processed in exactly the same way. Since the statistical accuracy for the  $^3\text{He}(\vec{d}, \vec{p})$  runs was much higher, the discussion which follows will be illustrated by spectra from those runs, it being understood that everything said about the protons from  $^3\text{He}(\vec{d}, \vec{p})$  applies equally well to the n-p recoil protons produced by the neutrons from  $^2\text{H}(\vec{d}, \vec{n})$ .

### D. Data analysis

The availability of the seven parameters and tag word made it possible to generate a variety of two-dimensional spectra and study correlations between the various parameters. Further, various gates could be applied so as to examine correlations between any two parameters in terms of selected values for the other parameters. The essential features of the analysis procedure were as follows. First, the data were sorted into four groups,  $L\uparrow$ ,  $L\downarrow$ ,  $R\uparrow$ , and  $R\downarrow$ , where  $L\uparrow$ , for example, is the yield of left-scattered protons with incident deuterons of  $\uparrow$  spin orientation. Then,  $t3_{\text{bot}}$  and  $t3_{\text{top}}$  signals were replaced by the average  $t3 = \frac{1}{2}(t3_{\text{bot}} + t3_{\text{top}})$  for improved  $t3$  resolution. A raw two-dimensional plot of  $t1$  vs  $t2$  for the  $^3\text{He}(\vec{d}, \vec{p})$  reaction is shown in Fig. 3(a). The  $t1$  values show the TOF distribution of the  $^3\text{He}(\vec{d}, \vec{p})$  protons [which approximately mirrors the TOF distribution of neutrons from the  $D(\vec{d}, \vec{n})$  reaction] and  $t2$  the TOF of protons between  $S1$  and  $S2$ . The group in the upper left are the continuum breakup protons, the middle group is the monoenergetic

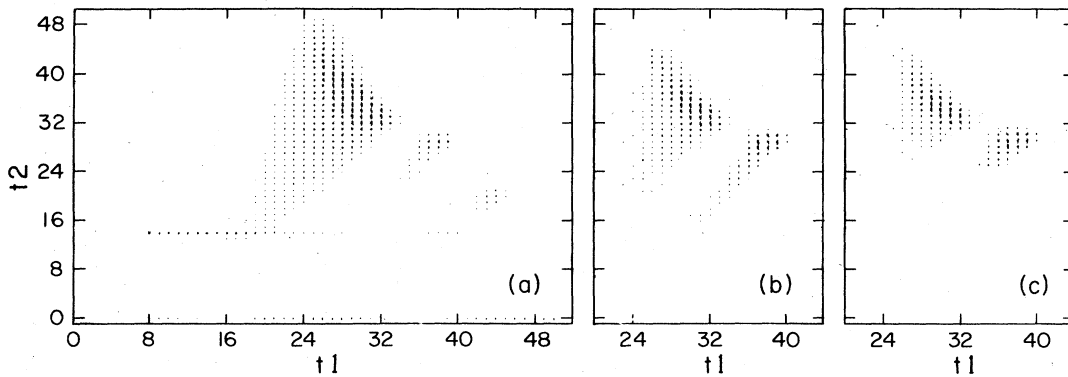


FIG. 3. Two-dimensional scatter plot of  $t_1$  vs  $t_2$  for the  ${}^3\text{He}(d,p)$  reaction. (a) Raw data without gates or cuts; (b) events within wide gate  $G_1$  on  $t_2$  [see Fig. 4(a)], and gate  $G_2$  on  $t_3$  (Fig. 5) and above threshold on  $E_3$  indicated by dashed line in Fig. 5; (c) final plot after exclusion of events to the right of dashed line in Fig. 4(b) and those outside gate  $G_3$  of Fig. 5. The events finally analyzed are the group on the right-hand side of the plot.

proton group from  ${}^3\text{He}(\vec{d}, \vec{p}){}^4\text{He}$ , and the small group at the lower right is attributed to events in which  $\gamma$  rays from the production target interact in  $T_1$  to produce relativistic electrons which are detected in  $S_2$  in accidental coincidence with pulses from  $S_3$ . Since the stop signal for  $t_1$  is generated by pickup from the cyclotron rf voltage, the resolution of the  $T_1$  spectrum reflects both the stability of the cyclotron and the inherent time structure of the beam micropulse. [In the analogous spectrum for the  ${}^2\text{H}(\vec{d}, \vec{n})$  neutrons, additional broadening would be caused by the energy-loss spread in  $T_1$ .]

Figure 4(a) shows the raw  $t_2$  vs  $E_2$  spectrum for the

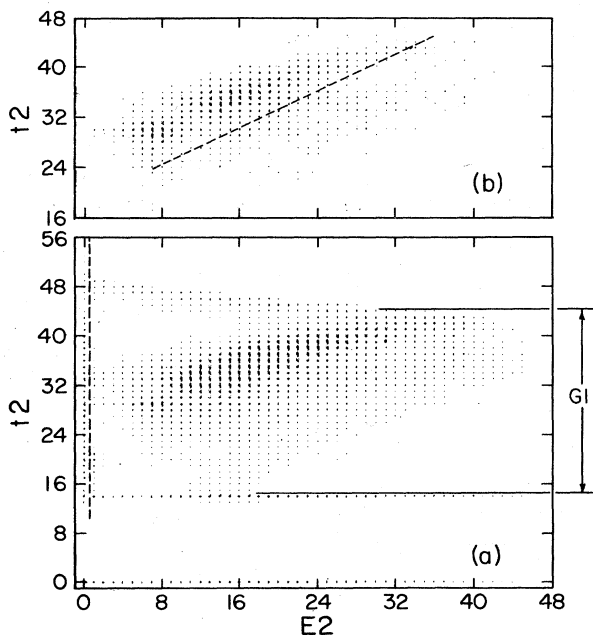


FIG. 4. Two-dimensional scatter plot of  $t_2$  vs  $E_2$  for the same data as in Fig. 3(a). (a) Raw data events without gates; (b) events passing the same gates and cuts as in Fig. 3(b).

same data. The main locus here has the shape of a side-wise "v." The protons of the high energy monoenergetic group are seen in the lower leg of the v, at about  $t_2=29$ . The heavy band of events sloping upward to the right are protons from the continuum breakup spectrum. The upper leg of the v, above about  $t_2=43$ , is due to low energy protons which stop in  $S_2$  (in accidental coincidence with pulses from  $S_3$ ). Finally, the raw spectrum of  $E_3$  vs  $t_3$  for the same data is shown in Fig. 5. The true triple coincidence events are in a narrow band about  $t_3=30$ . The broad continuum of lower pulse heights at other  $t_3$  values is entirely due to accidental coincidences, which amount to most of the data.

After much investigation of the effects of placing gates and thresholds on various parameters, the procedure adopted can be summarized as follows. The wide gate  $G_1$  was set on  $t_2$  [see Fig. 4(a)], to eliminate zeros and pedestal pulses from that time-to-amplitude converter (TAC) and to eliminate the accidental events in the upper leg of

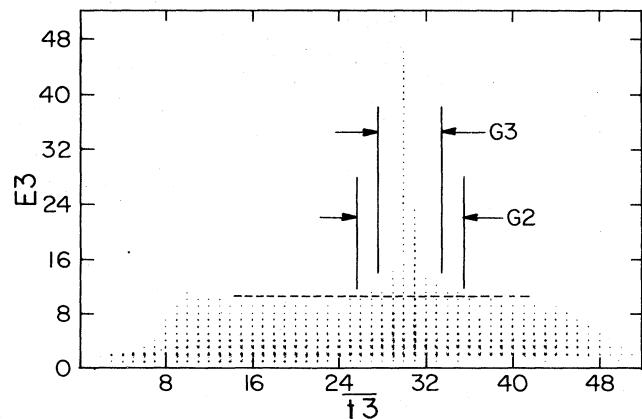


FIG. 5. Two-dimensional scatter plot of  $t_3$  vs  $E_3$  for the same data as in Fig. 3(a). The events below the  $E_3$  threshold indicated by the dashed line are almost entirely due to accidental coincidences.

the  $\nu$ . In addition, a threshold indicated by the dashed line in Fig. 4(a) was set on  $E2$ , primarily to eliminate events with  $E2=0$ . The gate  $G2$  was also set on  $t3$  (see Fig. 5) and the threshold shown by the dashed line was set on  $E3$ , so as to eliminate most of the events which were clearly accidental coincidences.

The result of this sifting of the data can be seen in Figs. 3(b) and 4(b). The spectra have been "cleaned up" considerably, and the peak due to  $\gamma$  rays has disappeared. Two features which remain, however, are in need of explanation. The band of events trailing off to the lower left from the monoenergetic peak in Fig. 3(b) is attributed to late start pulses to the  $t1$  TAC. These have the effect of reducing both  $t1$  and  $t2$  from their proper values. They occur when a pulse from  $S1$  is just below the  $S1$  discriminator threshold but is followed by an accidental pulse which adds enough light output to bring the  $S1$  pulse above that threshold. Since  $S1$  was a thin scintillator viewed from the edge, such an effect caused by inefficiency is not unexpected. There is no reason to eliminate such events. The other feature in need of explanation, seen in Fig. 4(b), is the large number of events to the right of the main locus in that figure. These are events in which the pulse height from  $S2$  is excessive and is attributed to p-p scattering in that scintillator, which would give rise to excessive pulse height. Since such events would diminish the effective analyzing power of the polarimeter it was decided to discriminate against them by excluding events to the right of the dashed line in Fig. 4(b). At the same time the narrower gate  $G3$  was set on  $t3$  (see Fig. 5). The final spectrum of  $t2$  vs  $t1$  is shown in Fig. 3(c), and counts in the monoenergetic peak of that spectrum were regarded as the true events. The crucial importance of the multiparameter data acquisition should be evident from the above discussion. Plots similar to Figs. 3–5 are not shown for the n-p data because their features are the same but their statistical accuracy was much lower.

The background measurements showed that the number of  $^{12}\text{C}(n,p)$  events was negligible in the multiparameter region where the n-p elastic scattering appeared, as expected from the large negative  $Q$  value of the reaction.

The desired scattering asymmetry was obtained by the ratio method through use of the formula

$$\epsilon(\text{np}) = \frac{r-1}{r+1}, \quad (3)$$

where

$$r = \left[ \frac{L \uparrow R \downarrow}{L \downarrow R \uparrow} \right]^{1/2}.$$

The polarization  $P_p(\text{np})$  of the n-p scattered protons was then given by the relation

$$P_p(\text{np}) = \frac{\epsilon(\text{np})}{A_p(\text{eff})}. \quad (4)$$

Finally, the polarization transfer parameter was calculated with the formula

$$D_t(179^\circ) = \frac{P_p(\text{np})}{P_n}. \quad (5)$$

#### IV. RESULTS AND DISCUSSION

The final weighted average of two separate measurements of  $D_t$  is  $-0.11 \pm 0.25$  at an effective center of mass scattering angle of  $179^\circ$ . Despite the relatively good absolute accuracy of the measurements, the fractional error in  $\epsilon(\text{np})$  is large [ $\epsilon(\text{np}) = -0.021 \pm 0.06$  for one data set]. Thus, while the measurement is not of sufficient accuracy to have impact on the phase shift analysis, it is in agreement with the phase shift predictions of the Virginia Polytechnic Institute-Texas A&M University-Michigan State University (VPI-TAMU-MSU) collaboration<sup>21</sup> (using the C 50 1983 solution) and in disagreement with the value of  $+0.7$  predicted by Gibbs and Stephenson. When the new data point was added to the data base, no significant changes were observed in the phase shifts. It has been estimated<sup>22</sup> that a measurement of  $D_t$  with an error  $\sim 0.05$  is needed before an appreciable effect on the phase shifts can be expected. This is a factor of 5 smaller than the error of the present measurement. Since the latter is almost entirely due to statistical uncertainties, an increase in yield by a factor of 25 would be needed to achieve the required precision. It is appropriate to speculate on how such an increase in yield might be obtained. Since the acquisition of final data for the present experiment consumed approximately two weeks of beam time, simply extending the running time is impractical. A factor of 4 could be gained by replacing the polyethylene target with a liquid-hydrogen target giving the same energy loss, with the side benefit of eliminating the background from the  $\text{C}(n,p)$  reaction. Another factor of 2 could be gained by making this target twice as thick. A factor of 5–10 could be gained by increasing the thickness of the neutron production target, either by increasing the length and pressure of the target cell or by replacing it with a liquid deuterium target. A factor of 5–10 could also be gained by increasing the beam intensity produced by the polarized ion source. The needed increase in yield would require several of these developments and most of them would be very costly in both money and effort, too costly to be implemented under present circumstances. The present experiment, however, is the first measurement of  $D_t$  for n-p scattering at moderate energies. While of insufficient accuracy to affect the phase shift analysis it has demonstrated the methods which could be used to obtain the required accuracy.

#### ACKNOWLEDGMENTS

We would like to thank M. J. Marolda and K. Washington for their assistance and help in the taking of the data, and the Cyclotron Institute staff for their support throughout this work. This work was supported in part by the National Science Foundation and by the U. S. Department of Energy.

- \*Present address: Fakultät für Physik, Albert Ludwig Universität, Freiburg, Federal Republic of Germany.
- †Present address: E-Systems, Inc., Greenville, TX 75401.
- <sup>1</sup>J. Binstock and R. Bryan, *Phys. Rev. D* **9**, 2528 (1974).
- <sup>2</sup>S. W. Johnson, F. P. Brady, N. S. P. King, M. W. McNaughton, and P. Signell, *Phys. Rev. Lett.* **38**, 1123 (1978).
- <sup>3</sup>R. J. N. Phillips, *Phys. Lett.* **1**, 19 (1963).
- <sup>4</sup>K. Gottfried and J. D. Jackson, *Nuovo Cimento* **34**, 735 (1964); G. A. Ringland and R. J. N. Phillips, *Phys. Lett.* **12**, 62 (1964).
- <sup>5</sup>W. R. Gibbs and G. J. Stephenson, private communication.
- <sup>6</sup>F. N. Rad, R. G. Graves, D. P. Saylor, M. L. Evans, E. P. Chamberlin, J. W. Watson, and L. C. Northcliffe, *Nucl. Instrum. Methods* **190**, 459 (1981).
- <sup>7</sup>E. P. Chamberlin and R. A. Kenefick, *Nucl. Instrum. Methods* **190**, 441 (1981).
- <sup>8</sup>W. D. Cornelius and R. L. York (unpublished).
- <sup>9</sup>R. L. York, J. C. Hiebert, H. L. Woolverton, and L. C. Northcliffe, *Phys. Rev. C* **27**, 46 (1983).
- <sup>10</sup>Y. K. Akimov, in *Scintillator Counters in High Energy Physics* (Academic, New York/London, 1965), p. 20.
- <sup>11</sup>The value of  $P^2I$  was computed from the values given in Tschalar *et al.*, *Nucl. Instrum. Methods* **78**, 141 (1970).
- <sup>12</sup>J. E. Simmons, W. B. Broste, G. P. Lawrence, J. L. McKibben, and G. G. Ohlsen, *Phys. Rev. Lett.* **27**, 113 (1971).
- <sup>13</sup>L. C. Northcliffe, W. D. Cornelius, J. C. Hiebert, and R. L. York (unpublished).
- <sup>14</sup>L. C. Northcliffe, W. D. Cornelius, R. L. York, and J. C. Hiebert, in *Polarization Phenomena in Nuclear Physics—1980 (Fifth International Symposium, Sante Fe)*, Proceedings of the Fifth International Symposium on Polarization Phenomena in Nuclear Physics, AIP Conf. Proc. No. 69, edited by G. G. Ohlsen, R. E. Brown, N. Jarmie, M. W. McNaughton, and G. M. Hale (AIP, New York, 1981), p. 1335.
- <sup>15</sup>R. L. York, W. D. Cornelius, L. C. Northcliffe, and J. C. Hiebert, in *Polarization Phenomena in Nuclear Physics—1980 (Fifth International Symposium, Sante Fe)*, Proceedings of the Fifth International Symposium on Polarization Phenomena in Nuclear Physics, AIP Conf. Proc. No. 69, edited by G. G. Ohlsen, R. E. Brown, N. Jarmie, M. W. McNaughton, and G. M. Hale (AIP, New York, 1981), p. 1461.
- <sup>16</sup>R. L. York, Ph.D. thesis, Texas A&M University, 1979, available from University Microfilms, Ann Arbor, MI.
- <sup>17</sup>H. O. Klages, H. Dobiasch, P. Doll, H. Krupp, M. Oexner, P. Plischke, B. Zeitnitz, F. P. Brady, and J. C. Hiebert, *Nucl. Instrum. Methods* **219**, 269 (1984).
- <sup>18</sup>S. Nath, R. G. Graves, J. C. Hiebert, L. C. Northcliffe, H. L. Woolverton, R. L. York, R. E. Brown, and P. Doleschall, *Phys. Rev. C* **28**, 2230 (1983).
- <sup>19</sup>R. M. Craig, J. C. Dove, G. W. Greenlees, J. Lowe, and D. L. Watson, *Nucl. Phys.* **79**, 177 (1966); **83**, 493 (1966).
- <sup>20</sup>S. Kato, K. Okada, M. Kondo, A. Shimizu, K. Hosono, T. Saito, N. Matsuoka, S. Nagamichi, K. Nishimura, N. Tamura, K. Imai, K. Egawa, M. Nakamura, T. Noro, H. Shimizu, K. Ogino, and Y. Kadota, *Nucl. Instrum. Methods* **169**, 589 (1980).
- <sup>21</sup>R. A. Arndt, L. D. Roper, R. A. Bryan, R. B. Clark, B. J. VerWest, and P. Signell, *Phys. Rev. D* **28**, 97 (1983).
- <sup>22</sup>B. Verwest, private communication.